A convenient one-pot synthesis, and characterisation of the ω-bromo-1-(4-cyanobiphenyl-4'-yl) alkanes (CBnBr)

Calum J Gibb, John MD Storey & Corrie T Imrie

Published online: 28 Jun 2022.

Submit your article to this journal ☐

Article views: 907

View related articles ☐

View Crossmark data ☐

Citing articles: 5 View citing articles ☐

Taylor & Francis
Taylor & Francis Group

A convenient one-pot synthesis, and characterisation of the ω-bromo-1-(4-cyanobiphenyl-4'-yl) alkanes (CBnBr)

Calum J Gibb, John MD Storey and Corrie T Imrie

Department of Chemistry, School of Natural and Computing Sciences, University of Aberdeen, Meston Building, Aberdeen, AB24 3UE, UK

ABSTRACT

A convenient synthetic route based on a sodium-mediated aromatic cross-coupling reaction is described for the multi-gram preparation of the ω-bromo-1-(4-cyanobiphenyl-4'−yl) alkanes (CBnBr, n = 2–10). These materials are not only key intermediates in the synthesis of oligomers and polymers but also exhibit fascinating liquid crystal behaviour in their own right. Nematic behaviour is observed for $n \geqslant 5$, and the nematic-isotropic transition temperature, T_{NI}, increases in essentially a linear manner on n. The properties of the ω-bromo-1-(4-cyanobiphenyl-4'−yloxy) alkanes (CBOnBr, n = 2–9) are also reported, and nematic behaviour is seen for $n \geqslant 3$. The values of T_{NI} show a weak odd-even effect on n in which the odd members show the higher values. The sense of this alternation is opposite to that seen for the 4-alkyloxy-4'-cyanobiphenyls, and this is attributed to the steric bulk of the bromine atom. The absence of smectic behaviour for both the CBnBr and CBOnBr series is attributed largely to electrostatic interactions that would arise from the concentration of the bromine atoms at the layer interfaces in an interdigitated smectic phase. A comparison of a range of cyanobiphenyl-based materials containing a chain with a terminal polar or polarisable group suggests that their phase behaviour is governed largely by their average molecular shapes.
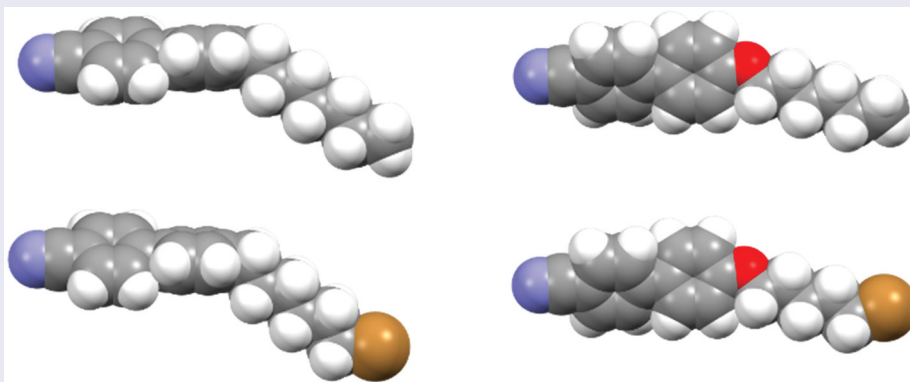
Introduction

Cyanobiphenyl is the most enduring of all mesogenic units. First discovered in the 1970s by Gray and his colleagues [1], the 4-alkyl and 4-alkyloxy-4"-cyanobiphenyls (Figures 1(a–b), respectively) were pivotal in the development of the liquid crystal display industry. The importance of cyanobiphenyl stretches far beyond this, however, and in the intervening fifty years it has been used in the design of a structurally diverse range of new liquid crystalline materials revealing new phase behaviour and underpinning new applications [2]. Most recently, the twist-bend nematic, N_{TB}, phase was first observed for the dimer, 1"7"-bis (4-cyanobiphenyl-4'−yl)heptane (CB7CB) [3–5]. A liquid crystal dimer consists of molecules containing two mesogenic units linked via a flexible alkyl spacer [6,7]. The N_{TB} phase quickly became the hottest topic in the field of liquid crystals, stimulating the synthesis and characterisation of a diverse range of odd-membered liquid crystal dimers many containing cyanobiphenyl (see, for example, [8–14]). The key structural requirement for a material to show the N_{TB} phase is molecular curvature and to achieve this, the odd-membered spacer is often attached to both mesogenic units by methylene links (see, for example, [8,15–18]). In a second group of twist-bend nematogens, the spacer is attached by

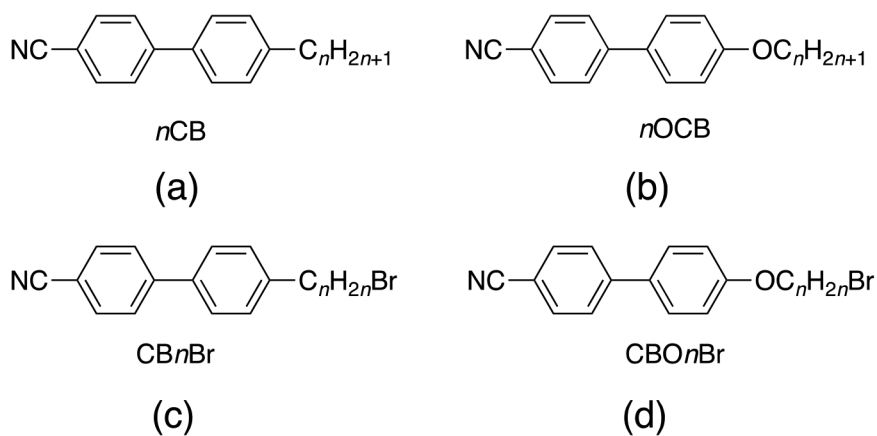CONTACT Corrie T Imrie ✉ c.t.imrie@abdn.ac.uk

Figure 1. The structures of the cyanobiphenyl-based series discussed, and the acronyms used to refer to them; in each, *n* denotes the number of carbon atoms in the terminal alkyl chain.

a methylene link to one mesogenic unit and by an ether link to the other, the most extensively studied example being 1-(4-cyanobiphenyl-4'-yloxy)-6-(4-cyanobiphenyl-4'–yl)hexane (CB6OCB) [19]. Synthetically, the introduction of the hexyloxy spacer allowed for the preparation of non-symmetric dimers having the appropriate molecular curvature to exhibit the N_{TB} phase [20,21] and led to the discovery of the twist-bend smectic phases [22–25]. A common synthetic intermediate in many of these materials is 1-bromo-1-(4-bromobiphenyl-4'–yl) hexane (BrB6Br) which is obtained by the Friedel Crafts acylation of 4-bromobiphenyl using 6-hexanoyl chloride to give 6-bromo-1-4'-bromo [11'–biphenyl]-4-yl)hexan-1-one and the subsequent reduction of this to yield BrB6Br. This is then used in a Williamson ether reaction to yield, for example, 1-(4-cyanobiphenyl-4"-yloxy)-6-(4-bromobiphenyl-4'–yl)hexane in the synthesis of CB6OCB, and the intermediate is subsequently cyanated using a modified Rosenmund Von-Braun reaction to yield the final product [19]. This synthetic route gives low overall yields, and its versatility is greatly restricted by the lack of availability of the ω-bromoalkanoic acids limiting the extent to which the spacer length may be varied.

These significant challenges may be circumvented by the availability of the ω-bromo-1-(4-cyanobiphenyl-4'–yl) alkanes (CB*n*Br), Figure 1(c), and these intermediates would expand the structure space accessible using straightforward chemistry with the expectation of enhancing our understanding of the fascinating family of twist-bend liquid crystal phases. Here, we present a convenient, one-pot synthesis for these key intermediates, the CB*n*Br series, and show that they are also materials of significant interest in their own right. Our approach is based on the chemistry developed by Panteleeva and co-workers for the preparation of cyanobiphenyl-based materials series

using sodium mediated aromatic coupling reactions (see, for example, [26–28]) and included the synthesis of 4CB and CB4Br but only in milligram quantities [29]. This methodology has much in common with the seminal work of Birch [30–32] and uses liquid ammonia as the solvent and activates the aromatic molecules through the addition of alkaline metals.

We compare the transitional behaviour of the CB*n*Br series with that of the ω-bromo-1-(4-cyanobiphenyl-4'–yloxy) alkanes (CBO*n*Br), Figure 1(d). These materials have been used in the preparation of a wide range of liquid crystalline materials including the nonsymmetric dimers leading to the discovery of the intercalated smectic phases [33–35], higher oligomers [36–39], and side-chain polymers [40–42]. The thermal behaviour of the CBO*n*Br series has been described recently by Davis *et al.* [43]. Apart from their key potential role as highly versatile synthetic intermediates, it should also be noted that the CB*n*Br series belongs to a general class of structures containing a polar or polarisable group at the terminus of an alkyl chain that attracts significant research interest having application potential in diverse areas including display applications [44,45] and chemo responsive sensors [46,47].

Experimental

Synthesis

The synthetic route used to obtain the CB*n*Br series is shown in Figure 2. The preparation of CB6Br is described as a representative example of the series. The method was identical for the other members of the series, and the quantities of reagents used, yields of the final products and their structural
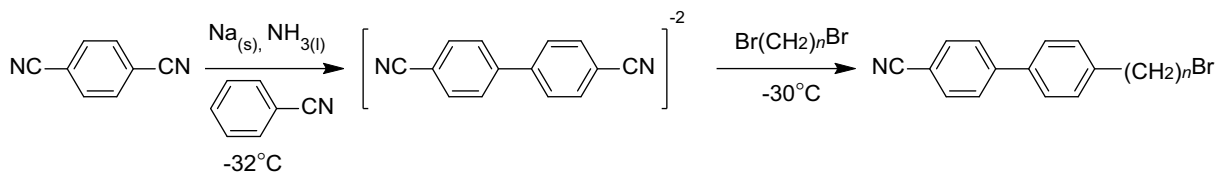
Figure 2. Synthetic scheme for the preparation of the CBnBr series.

characterisation data can be found in the Supplemental Information. The CBOnBr series was prepared as described in detail elsewhere [34,48], and their structural characterisation data are listed in the Supplementary Information.

Synthesis of 6-bromo-1-(4-cyanobiphenyl-4′–yl) hexane (CB6Br)

Terephthalonitrile (9.60 g, 75 mmol) was added to a flame-dried flask under an inert argon atmosphere. The flask was cooled to ca. −32 °C using an acetonitrile-dry ice bath, and filled with ammonia gas which condensed to give liquified ammonia (ca. 250 mL). Metallic sodium (3.5 g, 155 mmol) was added piecewise, and the reaction mixture turned dark brown as the anionic dinitrile benzene intermediate formed. After 10 min, and with constant stirring, nitrile benzene (11.60 g, 11.60 mL, 112.5 mmol) was added dropwise, and the reaction mixture stirred for 1.5 h. 1,6-Dibromohexane (21.95 g, 14.00 mL, 90.0 mmol) was added dropwise, and the reaction mixture left to stir for a further 2 h while carefully maintaining the temperature of the cooling bath at −30 °C. Diethyl ether (150 mL) was added slowly, maintaining the temperature of the cooling bath below −30 °C. After this addition, the flask was opened to the atmosphere, and the ammonia allowed to evaporate slowly as the bath approached room temperature. Distilled water (300 mL) was added, and the organic and aqueous layers separated. The aqueous layer was washed with diethyl ether (3 × 50 mL). The organic layers were combined, filtered, dried over anhydrous MgSO$_4$, and concentrated under reduced pressure to obtain a yellow oil. The crude product was purified by flash chromatography using a biotage selekt flash system utilising a step gradient with mixtures of diethyl ether:hexane as the eluent. CB6Br and nitrile benzene have almost indistinguishable retention times, and as a result coelute. The mixture obtained from the column was added to heptane over ice, and the desired product precipitated as a white solid. This was collected by filtration and recrystallised from MeOH in the form of white needles.

Yield 11.73 g, 46%. M.p. 48.2 °C.

IR (v, cm^{-1})2933, 2857 (sp^2 C-H stretch); 2220 (C≡N); 1604, 1474 (Ar-C=C); 812 (sp^2 C-H bend)

^{1}H NMR (400 MHz, Chloroform-d) (δ) 7.75–7.63 (m, 4 H, Ar-**H**), 7.51 (d, $J = 8.2$ Hz, 2 H, Ar-**H**), 7.29 (d, $J = 7.9$ Hz, 2 H, Ar-**H**), 3.41 (t, $J = 6.8$ Hz, 2 H, CH$_2$-**CH$_2$**-Br), 2.67 (t, $J = 7.7$ Hz, 2 H, Ar-**CH$_2$**-CH$_2$), 1.87 (p, $J = 6.9$ Hz, 2 H, CH$_2$-**CH$_2$**-CH$_2$-Br), 1.67 (p, $J = 7.6$ Hz, 2 H, Ar-CH$_2$ -**CH$_2$**-CH$_2$), 1.55–1.44 (m, 2 H, CH$_2$-**CH$_2$**-CH$_2$), 1.44–1.33 (m, 2 H, CH$_2$-**CH$_2$**-CH$_2$).

^{13}C NMR (101 MHz, CDCl$_3$) (δ) 145.57, 143.40, 136.58, 132.57, 129.18, 127.49, 127.13, 119.04, 110.58, 35.46, 33.92, 32.70, 31.14, 28.37, 28.00.

MS (QTof +): 364.0677 (100%, C$_{19}$H$_{20}$N^{23}Na, M + Na).

Materials

The structures of the products were determined using ^{1}H and ^{13}C NMR spectroscopies and FT-IR spectroscopy. NMR was performed using a 400 MHz Bruker Avance III HD NMR spectrometer and the IR spectra were recorded using a Thermal Scientific Nicolet IR100 FTIR spectrometer with an ATR diamond cell. Mass spectra were obtained using a Waters G2QTof Mass Spectrometer.

Characterisation

Characterisation of the transitional properties of the CBnBr and CBOnBr series were determined by differential scanning calorimetry using a Mettler Toledo DSC3 differential scanning calorimeter equipped with a TSO 801RO autosampler and calibrated using an indium standard. Samples were measured under a nitrogen atmosphere with 10 °C min^{-1} heating and cooling rates. The transition temperatures and entropy values reported are averages obtained for duplicate runs and normally extracted from heating traces. Phase identification was performed by polarised optical microscopy using an Olympus BH2 polarised optical microscope equipped with a Linkam TMS 92 heating stage. Samples were viewed between untreated glass slides.

Molecular modelling

Quantum mechanical density functional theory (DFT) calculations at the B3LYP 6-31 G(d) level of theory have been performed for all members of the CB*n*Br and CBO*n*Br series using Gaussian09 software [49]. Optimised geometries, molecular dipole moments and electrostatic potential surfaces were calculated, and visualised using GaussView 5 [50] Space-filling and ball-and-stick models were produced from the optimised geometry using Mercury 4.0 [51].

Results and discussion

We have described a one-pot synthetic methodology for the multi-gram scale synthesis of the ω-bromo -1-(4-cyanobiphenyl-4'–yl) alkanes (CB*n*Br). This sodium mediated aromatic cross-coupling method provides a more efficient and greener route to these materials than that previously described, [22] and for the first time makes these highly versatile intermediates readily available for a range of alkyl chain lengths. A minor side product of this synthetic approach is the corresponding CB*n*CB dimer although we have not quantified this. We have, however, by appropriately varying the quantities of the reagents used obtained CB7CB as the major product of the reaction with the overall yield being comparable to that seen for CB7Br.

The transitional properties of the CB*n*Br series are listed in Table 1. The shorter members of the series, $n = 2$–4, show the highest melting points and do not exhibit liquid crystallinity. For the remaining members of the series, with the exception of the octyl homologue, a monotropic nematic phase is observed. All the nematic phases described here were identified on the basis of the observation of a characteristic schlieren optical texture containing both types of point singularity and which flashed when subjected to mechanical stress; a representative schlieren texture is shown in Figure 3. The values of the entropy changes associated with the
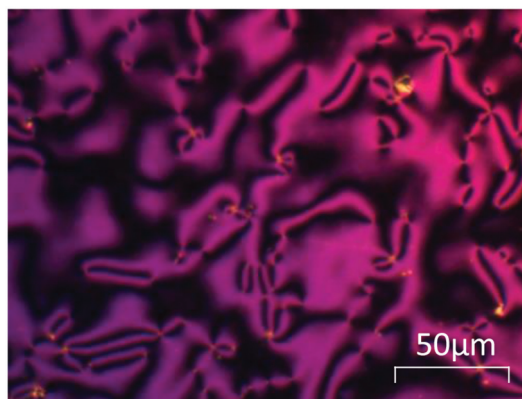

Figure 3. (Colour online) The nematic schlieren texture observed for CB10Br at 38 °C.

nematic-isotropic transition listed in Table 1 are wholly consistent with these assignments [52]. A value of the nematic isotropic transition temperature, T_{NI}, was estimated for the octyl homologue using a phase diagram constructed for binary mixtures of CB8Br and 5CB (Figure S1).

The melting points of the CB*n*Br series show an odd-even effect as *n* is increased in which the even members have the higher values, see Figure 4. The initial large fall in the melting points on increasing *n* allows the monotropic nematic phase to be observed for the longer members of the series. Indeed, CB7Br is a room temperature monotropic nematogen that has not crystallised over a period of months. The values of T_{NI} for the

Table 1. Transition temperatures and associated scaled entropy changes for the CB*n*Br series.

n	T_{Cr-}/°C	T_{NI}/°C	$\Delta S_{Cr-}/R$	$\Delta S_{NI}/R$
2	129.6		5.6	
3	71.5		7.5	
4	77.1		5.9	
5	39.8	19.2	8.3	0.13
6	48.2	22.5	7.8	0.19
7	32.7	26.2	8.2	0.20
8	59.0	[30.5]†	10.9	
9	36.7	34.3	11.1	0.27
10	60.7	38.0‡	13.5	

Note: †Virtual transition temperature estimated using a binary phase diagram with 5CB.

Note: ‡Measured using polarised light microscopy.

Figure 4. (Colour online) The dependence of the melting temperatures on the length of the terminal chain, *l*, for the CB*n*Br (circles), CBO*n*Br (squares), *n*CB (triangles) and *n*OCB (diamonds) series. For the methylene-linked chains $l = n$, and for the ether-linked chains $l = n + 1$.
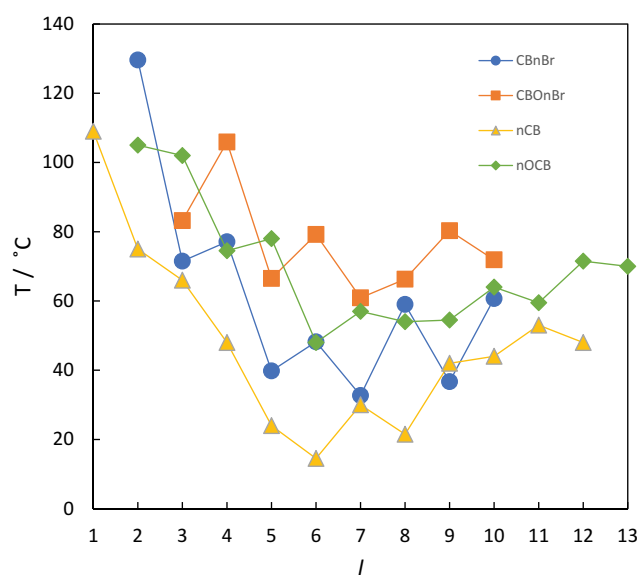
Figure 5. (Colour online) The dependence of the clearing temperatures on the length of the terminal chain, l, for the CBnBr (circles), CBOnBr (squares), nCB (triangles) and nOCB (diamonds) series. For the methylene-linked 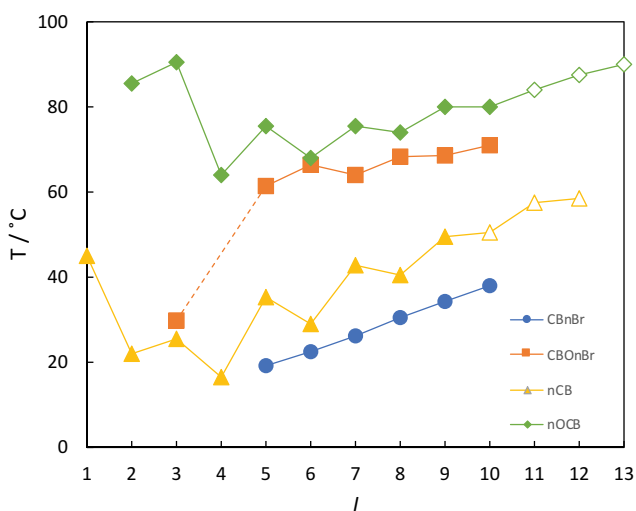chains $l = n$, and for the ether-linked chains $l = n + 1$. Filled symbols denote N-I transitions and open symbols SmA-I transitions.

CBnBr series increase in essentially a linear fashion on increasing n (Figure 5), and we will return to this surprising observation later.

The transitional properties of the CBOnBr series are listed in Table 2. A nematic phase was observed for all the members of the series with the exception of CBO3Br for which no liquid crystalline behaviour was observed. The scaled entropy changes associated with the nematic-isotropic transitions are consistent with these assignments. The values of T_{NI} listed in Table 2 show reasonable agreement with those reported by Davis *et al.* [43]. The most significant difference in the values of T_{NI} is for CBO9Br for which the value listed in Table 2 is 12.4°C higher than that reported previously. The melting points of the CBOnBr series also initially show an odd-even effect on increasing n in which the odd members tend to show the higher values, see Figure 4. The values of T_{NI} show a large increase on passing from n = 2 to 4 of 31.6°C. Attempts to obtain a virtual value of T_{NI} for CBO3Br by constructing a phase diagram with 5CB

Table 2. Transition temperatures and associated scaled entropy changes for the CBOnBr series.

n	T_{Cr}/°C	T_{NI}/°C	ΔS_{Cr}/R	ΔS_{NI}/R
2	83.2	29.8	6.8	0.09
3	105.9	-	6.7	
4	66.5	61.4	6.8	0.08
5	79.2	66.4	8.1	0.15
6	60.9	64.0	12.1	0.16
7	66.3	68.3	10.2	0.18
8	80.2	68.6	11.4	0.17
9	71.9	71.0‡	10.9	

Note: ‡Measured using polarised light microscopy.

were unsuccessful. On increasing n further from 4 to 9 sees T_{NI} rise by just 9.6°C, and superimposed upon this is a weak odd-even effect in which odd members show the higher values, see Figure 5.

Figures 4 and 5 compare the melting points and clearing temperatures, either nematic-isotropic or smectic A-isotropic transition temperatures, of the CBnBr, CBOnBr, nCB and nOCB series, respectively. In order for these comparisons to be meaningful, they are based on the total length of the terminal chain, l, such that $l = n$ for the methylene-linked chains, and $l = n + 1$ for the ether-linked chains to allow for the oxygen atom. As noted earlier, the melting points of the CBnBr and CBOnBr series tend to alternate on increasing n, and those of the latter series are higher for a given value of l. It is interesting to note that the senses of these alternations when plotted against l are the same. The dependence of the melting points of the nCB and nOCB series on l is less regular, but those of the latter series are also the higher of the two. For both pairs of series, the higher melting points seen for the ether-linked materials may be attributed to both the increased dipolar interactions arising from the ether-links, and also the enhanced packing efficiency arising from the relative disposition of the chain with respect to the cyanobiphenyl unit. For an ether-link, the chain lies more or less in plane with the mesogenic unit whereas for a methylene-link, the chain protrudes at an angle. The odd-even effect seen for the melting points of the CBnBr and CBOnBr series suggests that the relative disposition of the bulky bromine atom also affects packing efficiency and we will return to this theme later. It is noteworthy that the introduction of the bromine atom tends to increase the melting point when comparing the corresponding pairs of these four series.

Figure 5 reveals that the values of the clearing temperature of these four series are more clearly separated than their melting points. It is immediately apparent that the addition of the bromine atom reduces the value of the clearing temperature in both pairs of series, and that for any given value of l, the clearing temperature increases in the order:

$$CBnBr < nCB < CBOnBr < nOCB.$$

The average increase in the clearing temperature on moving from a member of the nCB to nOCB series for l = 6–10 is 33 °C and for the CBnBr and CBOnBr series is around 38°C. As described earlier, a terminal alkyloxy chain lies in the plane of the mesogenic unit to which it is attached whereas an alkyl chain protrudes at some angle, and this change in shape accounts to a large extent for the difference in clearing temperature. Furthermore, these data suggest that the terminal

bromine atom has little, or essentially no, additional effect on this difference in average shape between the methylene- and ether-linked materials given the similarity in the difference in clearing temperatures between the two corresponding sets of materials. The average difference between the values of T_{NI} for corresponding members of the CBOnBr and nOCB series for n = 4–9 is 9 °C. The same comparison for the CBnBr and nCB series, for n = 5–10, reveals a similar average reduction of 13 °C. Strictly for CB10Br and 10CB we are comparing differing phase transitions, and specifically, the former shows a nematic-isotropic transition whereas the latter exhibits a smectic A-isotropic transition. For the majority of liquid crystal series, however, the smectic-isotropic transition temperatures may be obtained by extrapolation of the nematic-isotropic transition temperatures [34]. Indeed, this appears to be the case here, and the inclusion of these data points make essentially no difference to the average reduction based only on the values of T_{NI}. Davis et al. suggested that this reduction in the clearing temperature between the nOCB and CBOnBr series arises from a combination of the steric bulk of the bromine atom and its polarity [43]. It is noteworthy that the value of T_{NI} for CBO2Br is 61 °C lower than that of 2OCB, a substantially larger reduction than seen for the longer members of the series, and we discuss this later.

The clearing temperatures of both the nCB and nOCB series show an odd-even effect on increasing n, see Figure 5. The effect of increasing the terminal chain length on the nematic-isotropic transition temperature, T_{NI}, for a liquid crystal series is two-fold [15,53]: on one hand, this increases the structural anisotropy of the molecule, and serves to increase T_{NI}. This change in the structural anisotropy depends on the number of atoms in the chain. For a methylene-linked chain, for example, adding a methylene unit to an even-membered chain increases the structural anisotropy to a greater extent than adding a methylene unit to an odd-membered chain because, in the former example, the additional methylene unit lies more or less parallel to the major molecular axis whereas in the latter case, it lies at an angle to this axis giving a smaller increase in structural anisotropy. This alternating shape gives rise to the observed odd-even effect superimposed on the underlying increase in T_{NI}. Counteracting this effect, however, is the increased dilution of the interactions between the mesogenic units arising from the increase in the mole fraction of alkyl chains within the system, and this serves to decrease T_{NI}. The overall effect of increasing the terminal chain length on the T_{NI} depends, therefore, on the interaction strength parameter between the mesogenic units. For three ring systems such

as terphenyl-based materials [53], the dilution effect dominates and T_{NI} decreases normally without alternation on increasing terminal chain length. By contrast for more weakly interacting mesogenic units, the enhanced structural anisotropy arising from increasing the terminal chain lengths dominates, and T_{NI} increases. Superimposed on this increasing trend is an odd-even effect reflecting the relative change in structural anisotropy governed by the parity of the chain. Such behaviour is clearly evident in Figure 5 for the nOCB, nCB and CBOnBr series. This interpretation of the odd-even effect on increasing the terminal chain length predicts that the sense of the alternation should be opposite for the nCB and nOCB series as n is increased because the oxygen atom may be considered analogous to a methylene unit. In Figure 5, the alternations for the two series are in the same sense because the clearing temperatures are plotted against l, and the oxygen atom is effectively being considered as a methylene unit such that for the same value of l, the terminal methyl group in (n + 1)CB and nOCB molecules have essentially the same relative disposition with respect to the molecular long axis. By contrast, the values of T_{NI} for the CBOnBr series show an odd-even effect in which the alternation is in the opposite sense, see Figure 5, and this was not reported previously [43]. This suggests that the terminal bromine atom is contributing to the average molecular shape in a manner similar to a methyl group, see Figure 6, and the alternation in T_{NI} reflects the bromine atom moving on and off the long molecular axis as n increases. The Van der Wall's volume of the bromine atom is 14.40 cm^3 mol^{-1} and that of a methyl group is 13.67 cm^3 mol^{-1} [54]. To a first approximation, this increased steric bulk may account, at least in
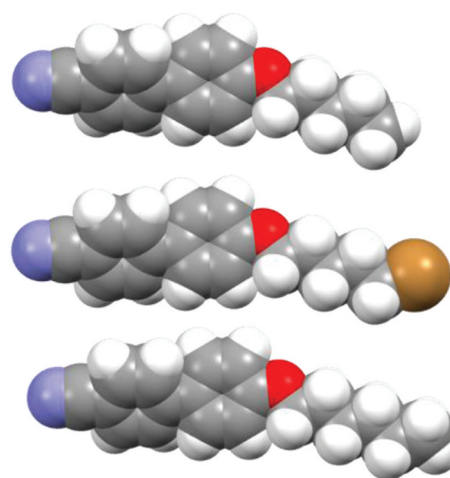

Figure 6. (Colour online) The molecular shapes of 5OCB (upper), CBO5Br (middle) and 6OCB (lower).

part, for the reduction in T_{NI} associated with the insertion of the bromine atom as suggested by Davis et al [43], but this simple comparison does not fully capture the change in molecular shape arising from the bromine atom and a more complete understanding must await such an analysis. Indeed, this observation also suggests that the polarity associated with the bromine atom, in fact, plays only a minor role in determining T_{NI}. It is interesting to note, however, that the behaviour seen in Figure 5 appears not to be a general observation, and in the odd-even effect seen for the values of T_{NI} shown by the ω-bromo -1-(4-methoxyazobenzene-4'−oxy)alkanes, the even members show the higher values suggesting that the terminal bromine group is not acting as a methyl group [52]. The physical significance of this differing behaviour is not clear.

Quite differing behaviour is seen for the values of T_{NI} for the CB*n*Br series as *n* is increased (Figure 5), and we have already noted that these increase in essentially a linear fashion. By comparison, those of the *n*CB series show an odd-even effect in which the odd members have the higher values as would be expected. This behaviour suggests that for the CB*n*Br series the structural anisotropy simply increases monotonically on increasing *n*, although we can offer no explanation for this highly unusual behaviour.

A striking feature of Figure 5 is the much lower value of T_{NI} observed for CBO2Br than for 2OCB by 61°C. We have now seen that a more appropriate comparison may be with 3OCB, and the reduction in T_{NI} passing to CBO2Br is 34°C, still much larger than the average found for the remaining members of the series of just 9°C. Figure 7 shows the electrostatic potential surfaces, space filling models and dipole moments for both CB2OBr and 3OCB. The larger reduction in T_{NI} seen
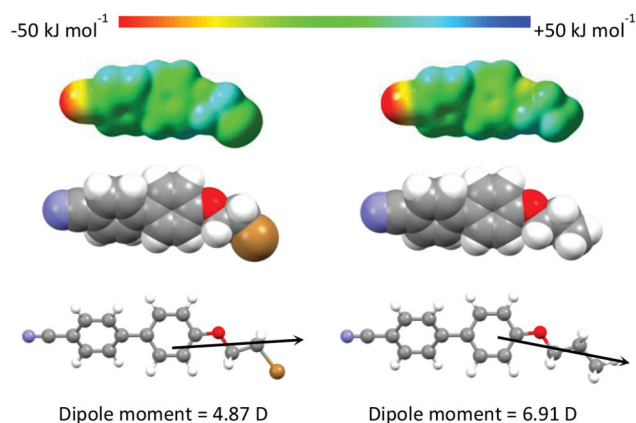

Figure 7. (Colour online) The electrostatic potential surfaces (top), space filling (middle) and ball-and-stick models showing the molecular dipole moment (bottom) of CBO2Br (left) and 3OCB (right).

between this pair of materials than for those with longer chains may be associated with the larger relative effect of the bulky bromine atom on the shape of these smaller molecules. There is a significant difference in the molecular dipole moment between these molecules but this would also be the case for corresponding pairs of molecules with the same value of *n*. It is apparent that in CBO2Br the methylene chain is more electron deficient than in 3OCB, and this difference was also highlighted by Davis *et al.* [43]. It is possible that this contributes to the much lower value of T_{NI} seen for CBO2Br compared to the longer members of the series.

A dramatic difference between the CB*n*Br and CBO*n*Br series, and the *n*CB and *n*OCB series is the absence of smectic behaviour for the former pair. For example, 10CB and 10OCB both exhibit smectic A-isotropic transitions whereas CB10Br and CBO10Br are exclusively nematogenic. In this respect, these materials differ significantly to other systems reported for which the incorporation of a halogen atom in a terminal chain actually promotes smectic behaviour including, for example, difluoroterphenyl-based [55] and 2-phenylpyrimidine-based materials [44]. These systems contain two terminal chains, only one of which has a terminal halogen atom. The promotion of smectic behaviour has been interpreted in terms of either strong polar interactions at the interface stabilising the smectic layers [55], or alternatively, to the electron withdrawing effect of the halogen terminal group reducing the electrostatic repulsive interactions between the alkyloxy chains [44]. We note that it is not immediately apparent why these effects do not appear to operate for these cyanobiphenyl-based systems. The destabilisation of smectic behaviour is not only observed for the CB*n*Br and CBO*n*Br series but also for the corresponding chlorine [43] and fluorine [46] substituted materials. This difference in behaviour between the cyanobiphenyl-based systems and, for example, the difluoroterphenyl-based compounds [55] may be attributed to the strong tendency of cyanobiphenyl-based materials to form anti-parallel correlations in order to minimise dipolar energy giving rise to interdigitated smectic phases. This would concentrate the terminal bromine atoms at the same layer interfaces whereas in a monolayer structure composed of molecules containing two terminal chains, only one of which possesses a bromine substituent, the same number of bromine atoms are distributed equally over two interfaces. This concentration of the bromine atoms presumably results in unfavourable electrostatic interactions destabilising the formation of smectic layers. We note, however, that mixtures of CBO8Br and 8OCB only show smectic behaviour at high concentrations of 8OCB [43] whereas

our interpretation of smectic phase suppression would suggest that the mixtures should exhibit smectic behaviour over a broader range of composition. This now requires further study.

The dependence of T_{NI} on the nature of the terminal group in CB(O)nX materials has most often been discussed in terms of the effect of X on the dipolar properties of the compound. An alternative approach to account for the difference in behaviour arising from the chemical nature of X is to consider its effect on structural anisotropy. To a first-order approximation, we can consider this in terms of the dependence of the values of T_{NI} for these compounds on the molar volume of X [54] and such a comparison is shown in Figure 8 for CBOnX with X = H, Br, Cl [43], F [46], OH [56], CN [47], CH=CH$_2$ [45], and CH$_3$. We note that in some instances different phase transitions are compared given that the higher homologues of the nOCB and nCB series show SmA-I transitions. These are, none the less, reasonable comparisons given that, as we noted earlier, within the majority of homologous liquid crystal series, the smectic-isotropic transition temperatures may be obtained from an extrapolation of the nematic-isotropic transition temperatures [34]. For all values of n, T_{NI} decreases on replacing H by F, and this is consistent with the larger F atom reducing the structural anisotropy. Exchanging F by Cl also leads to a reduction in T_{NI} for all values of n, but the extent by which T_{NI} falls is now smaller than would be expected simply on the increased molar volume of Cl. On moving from Cl to CH$_3$, the value of T_{NI} increases for all values of n despite the increase in molar volume associated with the methyl group. On replacing CH$_3$ by the larger Br, the value of T_{NI} again decreases for all values of n. For the CBOnCN materials, the values of T_{NI} are higher than those seen for the corresponding compounds having the smaller Br substituent. It is noteworthy that the iodine-containing compound, CBO11I, does not exhibit liquid crystallinity although its melting point is higher than those of CBO11Br and CBO11Cl, and may preclude the observation of a monotropic phase [57]. For the largest group considered in this selection of materials, X = CH=CH$_2$ [45], for shorter chain lengths T_{NI} is lower than seen for the corresponding CBOnCN materials but this difference is marginally inverted for $n = 7$. This behaviour reflects the importance not only of the size of the substituent, as described by its molar volume, but also of its effect on molecular shape [34]. The substituent X will both increase the molecular length and breadth of the molecule, and for example, an anisometric unit such as CN will enhance the structural anisotropy to a greater extent than a Br substituent which has a similar molar volume. Hence, we tend to see higher values of T_{NI} for the CBOnCN series than for the corresponding members of the CBOnBr series. We do note, however, that these temperatures may also be moderated, to some extent, by electronic effects, but to a large extent a consideration of average molecular shape appears to account for the changes in the values of the clearing temperature. The exception to this are the values of T_{NI} for the CBOnOH series which, for any given value of n, are the highest observed. This apparently counterintuitive behaviour may be attributed to hydrogen bonding and the formation of extended supramolecular
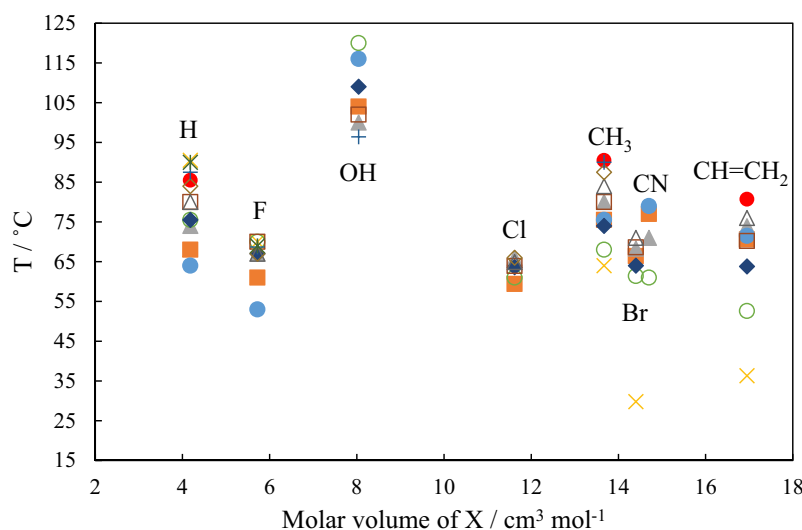

Figure 8. (Colour online) The dependence of the clearing (nematic-isotropic or smectic A-isotropic) temperature on the Van der Waal's volume of the group X for CBOnX materials with X = H, F [46], OH [56], Cl [43], CH$_3$, Br, CN [47], and CH=CH$_2$ [45]. The values of n are 1 (red circle), 2 (×), 3 (blue circle), 4 (open circle), 5 (orange square), 6 (navy diamond), 7 (grey triangle), 8 (open square), 9 (open triangle), 10 (open diamond), 11 (+), and 12 (�֎).

species. Even higher clearing temperatures have been observed for low molar mass materials containing terminal carboxylic acid groups [58].

Very similar trends in the values of T_{NI} are found for the corresponding but much smaller CBnX family of materials [46,47,56] although the value of T_{NI} reported for CB4F appears rather high and the molecular significance of this is not clear [46]. It is interesting to note that the values of T_{NI} are rather similar for the CBOnX materials with X = F or Br, whereas the difference appears larger between the corresponding CBnX systems. This supports the view that shape is the key factor because the substituent X contributes to a greater reduction in structural anisotropy for a CBnX molecule given that the chain protrudes out of the plane defined by the mesogenic unit.

For both the nCB and nOCB series smectic A phase behaviour emerges at $n = 8$, and for $n = 10–12$ nematic behaviour is extinguished and a SmA-I transition is observed. For all the corresponding CB(O) nX materials with n ≥ 8 (×=Br, Cl, F, OH) only nematic behaviour is observed. The only exception to this are the materials with X = CH=CH$_2$ for which smectic behaviour emerges at n = 8 [45]. The molecular significance of this strong suppression of smectic phase behaviour in this class of materials has to be established.

Conclusions

A one-pot synthetic methodology for the multi-gram scale synthesis of the ω-bromo-1-(4-cyanobiphenyl-4"−yl) alkanes (CBnBr) has been reported. Although not described here, we have also used this method to prepare the extensively studied 1",ω"-bis(4-cyanobiphenyl-4'−yl)alkanes, CBnCB, in a single-step, significantly simplifying published procedures [8]. The CBnBr and CBOnBr series show only nematic behaviour. The odd-even effect seen for the values of T_{NI} on increasing n for the CBOnBr series show what may be considered to be an inverted odd-even effect. This is attributed to the steric bulk of the bromine atom. By contrast, the values of T_{NI} for the CBnBr series increase essentially linearly on increasing n, and the physical significance of this difference in behaviour is not clear. It is clear that for cyanobiphenyl-based materials, a terminal halogen atom on the chain suppresses smectic behaviour in stark contrast to the behaviour of other types of systems in which a terminal halogen atom promotes smectic behaviour [44,55]. We suggest that this difference in behaviour arises not only for steric reasons but also stems from electrostatic interactions that may arise in an interdigitated smectic phase.

Disclosure statement

No potential conflict of interest was reported by the authors.

ORCID

Corrie T Imrie 🆔 http://orcid.org/0000-0001-6497-5243

References

[1] Gray GW, Harrison KJ, Nash JA. New family of nematic liquid-crystals for displays. Electron Lett. 1973;9:130–131.

[2] Dunmur DA. The magic of cyanobiphenyls: celebrity molecules. Liq Cryst. 2015;42:678–687.

[3] Cestari M, Diez-Berart S, Dunmur DA, et al. Phase behavior and properties of the liquid-crystal dimer 1 ",7"-bis (4-cyanobiphenyl-4'- yl) heptane: a twist-bend nematic liquid crystal. Phys Rev E. 2011;84:031704.

[4] Borshch V, Kim YK, Xiang J, et al. Nematic twist-bend phase with nanoscale modulation of molecular orientation. Nat Commun. 2013;4:2635.

[5] Zhu CH, Tuchband MR, Young A, et al. Resonant Carbon K-edge soft X-Ray scattering from lattice-free heliconical molecular ordering: soft dilative elasticity of the twist-bend liquid crystal phase. Phys Rev Lett. 2016;116:147803.

[6] Imrie CT, Henderson PA. Liquid crystal dimers and higher oligomers: between monomers and polymers. Chem Soc Rev. 2007;36:2096–2124.

[7] Imrie CT, Henderson PA, Yeap G-Y. Liquid crystal oligomers: going beyond dimers. Liq Cryst. 2009;36:755–777.

[8] Paterson DA, Abberley JP, Harrison WT, et al. Cyanobiphenyl-Based liquid crystal dimers and the twist-bend nematic phase. Liq Cryst. 2017;44:127–146.

[9] Abberley JP, Jansze SM, Walker R, et al. Structure-Property relationships in twist-bend nematogens: the influence of terminal groups. Liq Cryst. 2017;44:68–83.

[10] Mandle RJ, Archbold CT, Sarju JP, et al. The dependency of nematic and twist-bend mesophase formation on bend angle. Sci Rep. 2016;6:36682.

[11] Arakawa Y, Komatsu K, Ishida Y, et al. Carbonyl- and thioether-linked cyanobiphenyl-based liquid crystal dimers exhibiting twist-bend nematic phases. Tetrahedron. 2021;81:131870.

[12] Arakawa Y, Komatsu K, Tsuji H. Twist-Bend nematic liquid crystals based on thioether linkage. New J Chem. 2019;43:6786–6793.

[13] Cruickshank E, Salamonczyk M, Pociecha D, et al. Sulfur-Linked cyanobiphenyl-based liquid crystal dimers and the twist-bend nematic phase. Liq Cryst. 2019;46:1595–1609.

[14] Panov VP, Vij JK, Mehl GH. Twist-Bend nematic phase in cyanobiphenyls and difluoroterphenyls bimesogens. Liq Cryst. 2017;44:147–159.

[15] Forsyth E, Paterson DA, Cruickshank E, et al. Liquid crystal dimers and the twist-bend nematic phase: on the role of spacers and terminal alkyl chains. J Molec Liq. 2020;320:114391.

[16] Henderson PA, Imrie CT. Methylene-Linked liquid crystal dimers and the twist-bend nematic phase. Liq Cryst. 2011;38:1407–1414.

[17] Mandle RJ, Goodby JW. Dependence of mesomorphic behaviour of methylene-linked dimers and the stability of the N-TB/N-X phase upon choice of mesogenic units and terminal chain length. Chem: Eur J. 2016;22:9366–9374.

[18] Mandle RJ. Designing liquid-crystalline oligomers to exhibit twist-bend modulated nematic phases. Chem Rec. 2018;18:1341–1349.

[19] Paterson DA, Gao M, Kim YK, et al. Understanding the twist-bend nematic phase: the characterisation of 1-(4-cyanobiphenyl-4 '-yloxy)-6-(4-cyanobiphenyl-4'-yl)hexane (CB6OCB) and comparison with CB7CB. Soft Matter. 2016;12:6827–6840.

[20] Paterson DA, Crawford CA, Pociecha D, et al. The role of a terminal chain in promoting the twist-bend nematic phase: the synthesis and characterisation of the 1-(4-cyanobiphenyl-4 '-yl)-6-(4-alkyloxyanilinebenzylidene-4'-oxy)hexanes. Liq Cryst. 2018;45:2341–2351.

[21] Walker R, Pociecha D, Strachan GJ, et al. Molecular curvature, specific intermolecular interactions and the twist-bend nematic phase: the synthesis and characterisation of the 1-(4-cyanobiphenyl-4-yl)-6-(4-alkylanilinebenzylidene-4-oxy)hexanes (Cb6o.M). Soft Matter. 2019;15:3188–3197.

[22] Abberley JP, Killah R, Walker R, et al. Heliconical smectic phases formed by achiral molecules. Nature Commun. 2018;9:228.

[23] Salamonczyk M, Vaupotic N, Pociecha D, et al. Multi-Level chirality in liquid crystals formed by achiral molecules. Nature Commun. 2019;10:1922.

[24] Pociecha D, Vaupotic N, Majewska M, et al. Photonic bandgap in achiral liquid crystals-A twist on a twist. Adv Mater. 2021;33:2103288.

[25] Cruickshank E, Anderson K, Storey JMD, et al. Helical phases assembled from achiral molecules: twist-bend nematic and helical filamentary B-4 phases formed by mesogenic dimers. J Molec Liq. 2022;346:118180.

[26] Vaganova TA, Panteleeva EV, Shteingarts VD. Reductive activation of arenecarbonitriles for the reactions with some carbon-centered electrophiles: the reaction mechanisms and synthetic applications. Russian Chem Bull. 2008;57:768–779.

[27] Panteleeva EV, Bagryanskay IY, Sal'-Nikov GE, et al. The formation of dicyanoterphenyls by the interaction of terephthalonitrile dianion with biphenylcarbonitriles in liquid ammonia. Arkivoc. 2011;8:123–133.

[28] Panteleeva EV, Shchegoleva LN, Vysotsky VP, et al. Reductive activation of arenes, XVIII. Cyanophenylation of aromatic nitrites by terephthalonitrile dianion: is the charge-transfer complex a key intermediate? Eur J Org Chem. 2005;2005:2558–2565.

[29] Peshkov RY, Panteleeva EV, Wang CY, et al. One-Pot synthesis of 4 '-alkyl-4-cyanobiaryls on the basis of the terephthalonitrile dianion and neutral aromatic nitrile cross-coupling. Beilstein J Org Chem. 2016;12:1577–1584.

[30] Birch AJ. Reduction by dissolving metals .3. J Chem Soc. 1946;593–597.

[31] Birch AJ. Reduction by dissolving metals .4. J Chem Soc. 1947;102–105.

[32] Birch AJ. Reduction by dissolving metals. Part I. J Chem Soc. 1944;430–436.

[33] Hogan JL, Imrie CT, Luckhurst GR. Asymmetric dimeric liquid-crystals - the preparation and properties of the α-(4-cyanobiphenyl-4'-oxy)-ω-(4-n-alkylanilinebenzylidene-4 '-oxy)hexanes. Liq Cryst. 1988;3:645–650.

[34] Attard GS, Date RW, Imrie CT, et al. Nonsymmetrical dimeric liquid-crystals - the preparation and properties of the ?-(4-cyanobiphenyl-4'-yloxy)-ω-(4-n-alkylanilinebenzylidene-4'-o xy)alka. Liq Cryst. 1994;16:529–581.

[35] Imrie CT. Non-Symmetric liquid crystal dimers: how to make molecules intercalate. Liq Cryst. 2006;33:1449–1454.

[36] Imrie CT, Luckhurst GR. Liquid crystal trimers. The synthesis and characterisation of the 4,4 '-bis omega-(4-cyanobiphenyl-4'-yloxy)alkoxy biphenyls. J Mater Chem. 1998;8:1339–1343.

[37] Imrie CT, Lu ZB, Picken SJ, et al. Oligomeric rod-disc nematic liquid crystals. Chem Commun. 2007;1245–1247.

[38] Imrie CT, Stewart D, Remy C, et al. Liquid crystal tetramers. J Mater Chem. 1999;9:2321–2325.

[39] Tuchband MR, Paterson DA, Salamonczykc M, et al. Distinct differences in the nanoscale behaviors of the twist-bend liquid crystal phase of a flexible linear trimer and homologous dimer. Proc Natl Acad Sci, USA. 2019;116:10698–10704.

[40] Craig AA, Imrie CT. Effect of spacer length on the thermal-properties of side-chain liquid-crystal polymethacrylates .2. Synthesis and characterization of the poly omega-(4'-cyanobiphenyl-4-yloxy)alkyl methacrylates. Macromolecules. 1995;28:3617–3624.

[41] Imrie CT, Schleeh T, Karasz FE, et al. Dependence of the transitional properties of polystyrene-based side-chain liquid-crystalline polymers on the chemical nature of the mesogenic group. Macromolecules. 1993;26:539–544.

[42] Imrie CT, Karasz FE, Attard GS. Effect of backbone flexibility on the transitional properties of side-chain liquid-crystalline polymers. Macromolecules. 1993;26:3803–3810.

[43] Davis EJ, Mandle RJ, Russell BK, et al. Liquid-Crystalline structure-property relationships in halogen-terminated derivatives of cyanobiphenyl. Liq Cryst. 2014;41:1635–1646.

[44] Rupar I, Mulligan KM, Roberts JC, et al. Elucidating the smectic A-promoting effect of halogen end-groups in calamitic liquid crystals. J Mater Chem C. 2013;1:3729–3735.

[45] Mandle RJ, Goodby JW. An interplay between molecular pairing, smectic layer spacing, dielectric anisotropy and re-entrant phenomena in -alkenyloxy cyanobiphenyls. Liq Cryst. 2017;44:656–665.

[46] Wang KL, Rai P, Fernando A, et al. Synthesis and properties of fluorine tail-terminated cyanobiphenyls and terphenyls for chemoresponsive liquid crystals. Liq Cryst. 2020;47:3–16.

[47] Wang KL, Szilvasi T, Gold J, et al. New room temperature nematogens by cyano tail termination of alkoxy and alkyl-cyanobiphenyls and their anchoring behavior on metal salt-decorated surface. Liq Cryst. 2020;47:540–556.

[48] Crivello JV, Deptolla M, Ringsdorf H. The synthesis and characterization of side-chain liquid-crystal polymers based on polystyrene and poly-alpha-methystyrene. Liq Cryst. 1988;3:235–247.

[49] Frisch MJ, et al. Gaussian 09 (Revision B.01). Wallingford CT: Gaussian Inc.; 2010.

[50] Dennington R, Keith TA, Millam JMG. GaussView 5. 2009.

[51] Macrae CF, Sovago I, Cottrell SJ, et al. Mercury 4.0: from visualization to analysis, design and prediction. J Appl Crystal. 2020;53:226–235.

[52] Henderson PA, Cook AG, Imrie CT. Oligomeric liquid crystals: from monomers to trimers. Liq Cryst. 2004;31:1427–1434.

[53] Walker R, Pociecha D, Storey JMD, et al. Remarkable smectic phase behaviour in odd-membered liquid crystal dimers: the CT6O.M series. J Mater Chem C. 2021;9:5167–5173.

[54] Bondi A. Van der Waals volumes and radii. J Phys Chem. 1964;68:441–451.

[55] Goodby JW, Saez IM, Cowling SJ, et al. Transmission and amplification of information and properties in nanostructured liquid crystals. Angew Chem Int Ed. 2008;47:2754–2787.

[56] Wang KL, Jirka M, Rai P, et al. Synthesis and properties of hydroxy tail-terminated cyanobiphenyl liquid crystals. Liq Cryst. 2019;46:397–407.

[57] Mandle RJ, Davis EJ, Voll CCA, et al. Self-Organisation through size-exclusion in soft materials. J Mater Chem C. 2015;3:2380–2388.

[58] Stewart D, Imrie CT. Supramolecular side-chain liquid-crystal polymers .1. Thermal-behavior of blends of a low molar-mass mesogenic acid and amorphous polymers. J Mater Chem. 1995;5:223–228.